



## Complex networks description of ionosphere

Shikun Lu<sup>1,2</sup>, Hao Zhang<sup>1</sup>, Xihai Li<sup>2</sup>, Yihong Li<sup>2</sup>, Chao Niu<sup>2</sup>, Xiaoyun Yang<sup>2</sup>, and Daizhi Liu<sup>2</sup>

<sup>1</sup>Department of Electronic and Engineering, University of Tsinghua, Beijing, China.

<sup>2</sup>Xi'an Research Institute of Hi-Tech, Xi'an, China.

*Correspondence to:* Hao Zhang ([haozhang@mail.tsinghua.edu.cn](mailto:haozhang@mail.tsinghua.edu.cn))

**Abstract.** Complex networks have emerged as an important area of geoscience to generate novel insights into nature of complex systems. To investigate the information flow in ionosphere, the directed complex network is constructed based on the conditional independence theory. The results of the power-law hypothesis testing show that both the out-degree and in-degree distribution of the ionospheric network are not scale-free. The topological structure of the ionospheric information network is homogeneous. The spatial variation of the ionospheric network shows the connection principally exist between the neighbors in space, indicating that in ionosphere the information transmission is mainly based on the spatial distance. Moreover, the spatial edge distributions show that the information travels further along the latitude than along the longitude. Perhaps, this is because the dramatic variation of ionosphere along the geomagnetic field interrupts the information flow. Moreover, the analysis of small-world-ness shows the ionospheric information network is small-world, which may result from the current system in the ionosphere. The fractal analysis shows the ionospheric network is not self-organized, indicating the complexity of the spatial variation for long time in ionosphere.

*Copyright statement.* We confirm that this paper does not contain material, the copyright for which belongs to a third party.

### 1 Introduction

Complex networks have become an efficient tool to study the characteristics of complex systems, containing a large number of interacting parts. Their application spans in various scientific fields (Zerrenner et al., 2014), such as Biology (e.g. protein interaction networks), Information Technology (e.g. World Wide Web.), Social Sciences (e.g. social networks(Wang et al., 2016a, b)) etc. Including large numbers of irregularities with different sizes and affected by various factors (such as, solar irradiation, geomagnetic field, gravity wave and tidal wave(Kelly, 2009)), ionosphere performs as a complex system on the spatial and temporal variation. Hence, to characterize the complex dynamical features in space, the ionospheric data is mapped to a complex network.

Now, in modern statistical mechanics of geophysics, especially climate science (Nocke et al., 2015), the idea of complex network is receiving great attention. Donges et al. (2009a, b) used complex networks to uncover a backbone structure carrying a considerable amount of matter, energy, and dynamical information flow in the global surface air temperature field. Hlinka et al. (2013) investigated the reliability of directed climate networks detected by selected methods and parameter settings, using



a stationarized model of dimensionality-reduced surface air temperature data. Peron et al. (2014) investigated the temperature network of the North American region and showed that two network characteristics have marked differences between the eastern and western regions, which were a reflection of the presence of a large network community on the western side of the continent.

5 Another geophysical application of complex networks is about seismological science. Baiesi and Paczuski (2005) constructed directed networks of earthquakes by placing a link between pairs of events that are strongly correlated. Their results showed that the network was scale-free and highly clustered. Abe and Suzuki (2006) constructed growing random networks by the seismic data and found that these earthquake networks were scale-free and small-world. Jiménez et al. (2008) divided the Southern California region into cells of  $0.1^\circ$  and calculated the correlation of activity between them to create functional  
10 networks showing the small-world features. Suteanu (2014) proposed a network-based method for the assessment of earthquake relationships in space-time-magnitude patterns and results were further applied for the study of temporal changes in volcanic seismicity patterns. Furthermore, the complex network theory is also used in the study of other geoscience field, like rock fractures and cave passages (Phillips et al., 2015). On the ionosphere, the network theory was discussed by Podolská K. et.al. by two abstracts in 2010 and 2012 EGU General Assembly Conference (Podolská et al., 2010, 2012). However, the  
15 response email says the publications are still being prepared. The prior abstract wanted to study the correlations between main ionospheric parameters. The other one attempted to study the influence of geomagnetic disturbances and solar activity on thermal plasma parameters. So none of them tried to make complex networks description of ionosphere.

Matter, energy and information are called the three components of nature. In this article, we utilize directed complex networks to interpret ionospheric dynamical processes as information flow and describe its characteristics in ionosphere. Iono-  
20 spheric data supplied by the Centre for Orbit Determination in Europe (CODE) are selected. The article is organized as follows. The data and method description are provided in Section 2. Furthermore, the results about the patterns of the ionospheric information flow are presented in Section 3, finding that the network is homogenous and small-world for information transmission. The locally connected network is not length-scale invariant. Section 4 discusses the summary and conclusions.

## 2 Description of Data and Methods

### 25 2.1 VTEC Data Source

As a critical physical quantity of ionosphere, Vertical Total Electron Content(VTEC) carries abundant information about the climatological variation of ionosphere (Ercha et al., 2015). The International Global Navigation Satellite System Service (IGS) supplies global VTEC data with 2-hours time resolution. The dataset is determined from more than 200 IGS stations within a global scale (Wei et al., 2009). CODE, as one of 5 analysis centres of IGS, has estimated VTEC from the dual-frequency  
30 code and phase data of GPS since April 1998 (Guo et al., 2015). In the current research, VTEC data is derived from CODE (<ftp://ftp.unibe.ch/aiub/CODE>) in the form of Global Ionospheric Map(GIM). The GIM ranges from  $-180^\circ$  to  $180^\circ$  along the longitude and from  $-87.5^\circ$  to  $87.5^\circ$  along the latitude. The size of an elementary GIM cell is  $5^\circ$  along the longitude and  $2.5^\circ$  along the latitude. Each GIM cell is defined as a variable,  $x_{ij}(t)$ , where  $i$  and  $j$  indicate latitude and longitude coordinates of



latitude and longitude, and  $t$  is the universal time (UT). For the decrease of the computation by reducing the variables, the size of the GIM cells has been doubled. So the longitude and latitude resolution are  $10^\circ$  and  $5^\circ$ . Totally, the number of the variables (GIM cells)  $36 \times 36$ , which is 1296, because  $180^\circ$  and  $-180^\circ$  are the same for longitude. In this paper we select the data in 2012, so the data length of each variable is 4392.

## 5 2.2 Mapping the data to a probabilistic graph

As a complex system, the ionosphere is usually characterized by the presence of multiple interrelated aspects, which are caused by atmospheric waves, geomagnetic field and so on. The ionosphere, also involves a significant amount of uncertainty. Moreover, our observations are always noisy, even those aspects that are observed are often observed with some error. So, probability need to be used to represented such random property. As a result, probabilistic graph is selected to model the interrelation and uncertainty. We describe the ionospheric data as realization of a multivariate probabilistic graph on the global spatial grid.

Probabilistic graphs use a graph-based representation as the basis for compactly encoding a complex probabilistic distribution over a high-dimensional space (Koller and Friedman, 2009). Probability graph is a useful way of visualizing interactions between multiple variables. Therefore, in addition to inference, probabilistic graphs can also be used to discover the knowledge within the dataset. As complex networks, probabilistic graphs are constructed to represent a joint distribution by making conditional independence (CI) assumptions. The nodes in the networks represent random variables, and the edges represent CI assumptions (Murphy, 2012). The absence of an edge between two nodes implies that the corresponding random variables are conditionally independent given all other nodes. Based on the probability theory, we say  $X$  and  $Y$  are CI iff the conditional joint can be written as a product of conditional marginals:

$$20 \quad X \perp Y | Z \iff p(X, Y | Z) = p(X | Z)P(Y | Z) \quad (1)$$

As is known, the electric current is generated by the directed moving electric charge. Because of the existence of ionospheric current system, we believe the interaction between variables in ionosphere is directed. Moreover, as suggested in (Zerrenner et al., 2014), directed complex network can offer additional knowledge, like information transmission and the distinction between child and parent nodes. Thus, we can determine networks that only include directed edges between geographic locations in the ionospheric networks. As following, the construction of the directed ionospheric network, aka Bayesian probabilistic graph, is introduced to describe the information flow in global ionosphere. Conditional independence tests involving sets of variables can be used to determine the existence and direction of connections (i.e., the existence and direction of information flow)(Ebert?Uphoff and Deng, 2012).

As the metaphor shown in (Jie et al., 2002), we can view a Bayesian network as a information pipeline system, where nodes are valves which are connected by information channels (arcs). Information can flow through channels. Suppose two nodes,  $X$  and  $Y$ , are not directly connected (conditional independent) within the current network structure. There should be no information flow between these nodes after closing all of the existing indirect connections between  $X$  and  $Y$ . So the process

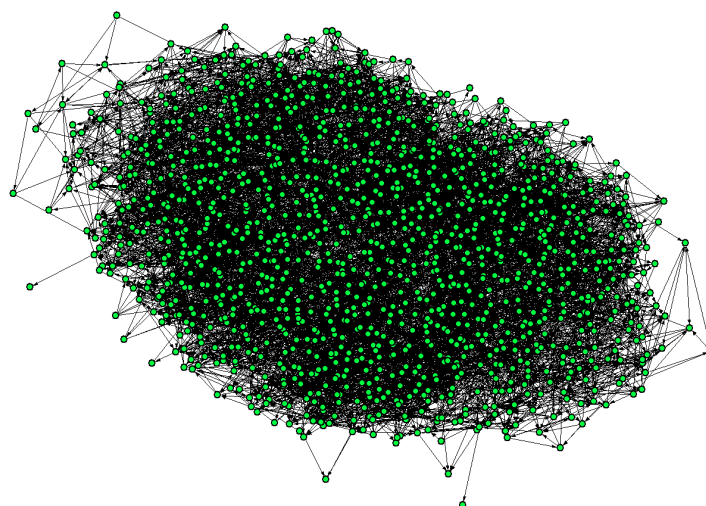


**Figure 1.** The directed complex network of ionosphere. The network is developed from the TEC dataset by the FGS algorithm. The 1296 green nodes indicate the global grid points, while the 10985 directed edges represent CI assumptions.

of conditional independence is performed via 'information flow'. Furthermore, the mathematical definition of information flow is shown in (Nihat and Daniel, 2011).

The network structure, i.e., which nodes are connected by an edge and directions of edges, is calculated using the Fast Greedy Equivalence Search (FGS) algorithm developed by Joseph Ramsey et.al. (Ramsey et al., 2017). We use the implementation of the FGS algorithm in the TETRAD package (Version 5.3.0-2, available at <http://www.phil.cmu.edu/projects/tetrad/>) and make the penalty discount is 10. The result is shown in Figure 1.

### 3 Results and Discussion

#### 3.1 Degree distribution of the ionospheric networks

As one of the most important parameter to depict the nodes, degree in a network is the number of connections the node has, and the degree distribution is the probability distribution of these degrees over the whole network. For directed network, the degree distribution is divided into two different kinds, the out-degree distribution, which is the distribution of outgoing edges, and the in-degree distribution, which is the distribution of incoming edges. The degree distribution of Figure 1 is shown in Figure 2.

It has been reported that real system networks often exhibit so called free-scale properties (Barabási and Albert, 1999). This means their degree distribution follows a power law, at least asymptotically. That is, the number of links  $k$  of a given node

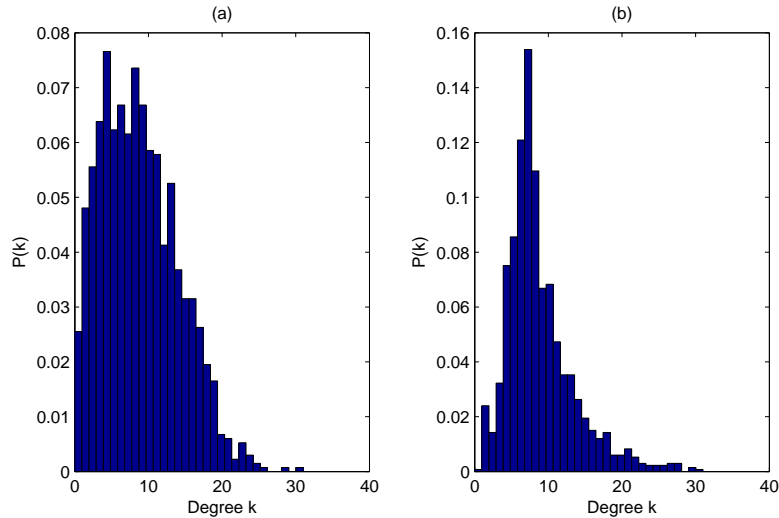


**Figure 2.** The degree distributions of the network of ionosphere. (a) is the out-degree distribution; (b) is the in-degree distribution.

exhibits a power law distribution  $P(k) \sim k^{-\gamma}$ , where  $P(k)$  can be calculated by the statistical frequency and  $\gamma$  is a parameter whose value is typically in the range  $2 < \gamma < 3$ . Form the distribution shown in Figure 2, it is hard to determine whether the observed degree is drawn from a power-law distribution or not. Clauset et al. (2009) presented a principled statistical framework for discerning power-law behavior in empirical data. As the method shown in (Clauset et al., 2009), we attempt to

5 test the power-law hypothesis quantitatively. Both the results of out-degree and in-degree reject the hypothesis, indicating that the ionospheric network is not a scale-free network. So, the topological structure of the ionospheric information network is homogeneous. There are no obvious 'hub' nodes in ionosphere. In other words, in the ionospheric information transmission, there is no distinctive spatial position performing as sources or attractors.

### 3.2 Spatial variation of the ionospheric network

10 Compared with the undirected probabilistic graph, the directed one can provide the additional knowledge about the information transmission within the network, providing an alternative viewpoint on the ionosphere. We particularly focus on the directed edges, which indicate the information flow in a network (Figure 1). In order to track these flow, we calculate the spatial distribution of edges based on the latitude and longitude difference between the beginning and end of directed edge. The result is shown in Figure 3. The positive differences represent the directions of edges are from west to east and from north to south.

15 As is shown in Figure 3, the nodes are connected mainly to their spatial neighbors. The local connections indicate that, in ionosphere the information flow transmission is mainly based on the spatial distance, the nearby principle. Furthermore, from the approximate symmetry along the Xlabel in Figure 3 (b) and (c), we can discover that, the information transposition are almost the same in the west and east (south and north) direction. From Figure 3(b) and (c), we can easily find that the number of edges decreases as the increase of the absolute value of latitude and longitude difference. In addition, comparing with the

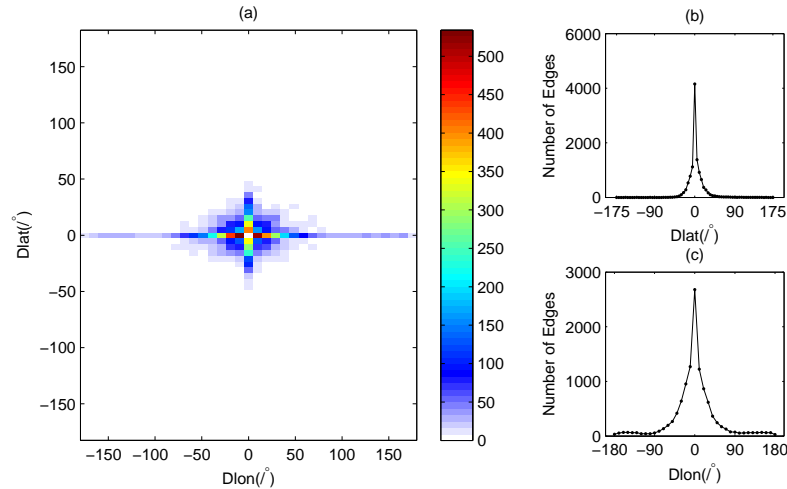


**Figure 3.** The global spatial distribution of directed edges. (a) is the joint distribution of edges against the differences of latitude and longitude; (b) is the distribution of edges against the difference of latitude; (c) is the distribution of edges against the difference of longitude.

standard deviations of the distribution shown in Figure 3(b) and (c), which are 16.42 and 50.51, the results show that the distribution curve along the latitude difference is more steep than that along longitude difference. Thus, the rate of decrease along the latitude difference is larger than that along the longitude difference. Accordingly, the information propagates further along the latitude than the longitude, which may be attributed to the orientation of geomagnetic field. Roughly speaking, the geomagnetic field travels meridionally with a small deflection. As is known, the moving electrons drift along the geomagnetic field line spirally. Therefore, the ionosphere changes more dramatically along the longitude than latitude, then, the fast information fading along longitude interrupts the information transmission.

Nevertheless, the ionospheric network is not completely connected locally. Long-range connections emerge both in the latitude and longitude direction. So the ionospheric network possess a basically ordered structure with some additional long-range connections, exhibiting the property of small-world.

### 3.3 Small-world structure of the ionospheric network

Lying between the completely random and completely regular network, the small-world network is a type of graph in which any given node are likely to reach every other node by a small number of steps comparing with the total number of network nodes (Gallo et al., 2007). The 'six degrees of separation' in social networks is one of the most famous examples. Watts and Strogatz (1998) found that some networks can be highly clustered, like regular lattices, yet have small characteristic path lengths, like random graphs. To investigate the small-world structure of the network, the original ionospheric has to be reduced to an undirected graph (Abe and Suzuki, 2006, 2009). Furthermore, to mathematically describe the small-world property, two



important measures are often selected, which are average clustering coefficient  $C$  and average shortest path length  $L$ . Their definitions are shown in Equation 2, 3 and 4.

$$C_i = \frac{2\Delta_i}{k_i(k_i - 1)}, \quad (2)$$

$$C = \frac{1}{N} \sum_{i=1}^N C_i, \quad (3)$$

$$L = \frac{2}{N(N-1)} \sum_{i \geq j} d_{ij}. \quad (4)$$

Here,  $C_i$  is the local clustering coefficient of node  $i$ .  $k_i$  is the degree of node  $i$  and  $\Delta_i$  denotes the number of edges between the neighbors of node  $i$  with node  $i$  itself excluded. The global clustering coefficient  $C$  is defined as the average of all local clustering coefficients  $C_i$ .  $N$  is the number of nodes and  $d_{ij}$  denotes the length of the shortest path between the nodes  $i$  and  $j$ .  $d_{ij}$  is calculated by Dijkstra algorithm (Newman, 2010). Thus,  $C$  describes the local connections, while  $L$  characterizes a network's connectivity structure globally (Zerenner et al., 2014).

To be quantitatively defined as a small-world network, values for two network properties must be compared with their values for the equivalent random graph, which has the same degree on average. A measurement of 'small-world-ness' is proposed as follows (Humphries and Gurney, 2008; Humphries et al., 2011):

$$\sigma = \frac{C/C_r}{L/L_r}, \quad (5)$$

where  $C$  and  $L$  are the average clustering coefficient and average shortest path length of the given network, while  $C_r$  and  $L_r$  are those of the the equivalent random network. If the given network fulfil the conditions,  $\sigma > 1$  and  $C/C_r > 1$ , it meet the small-world criteria. To reduce the impact of randomness, the results shown in Figure 4 is calculated by 150 random networks.

From Figure 4(a) and (c), we can easily find that the results all satisfy  $\sigma > 1$  and  $C/C_r > 1$ . Shown in Figure 4(b) and (d), the distributions are Gaussian, and the standard deviation are 0.028 and 0.035. The small standard deviations indicate the results are close to the real value, the averages 6.64 and 8.08. Therefore, the ionospheric graph behaves as a small-world network. In the ionospheric network, the small-world structure indicates that the information transmission may have short-cuts beyond the Euclidean distance. The long-range connections which might result from the current systems in the ionosphere.

### 3.4 Fractal nature of ionospheric networks

With the aim of providing a deeper understanding of the underlying mechanism within the ionospheric network, we investigate the fractal topology of the undirected complex network gotten in the prior Section. Song et al. (2005) applied a box covering

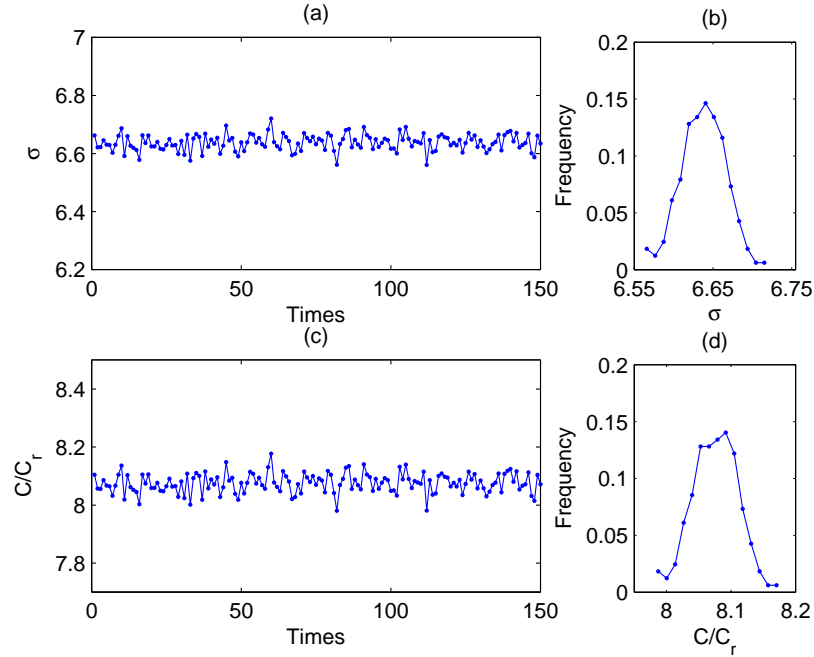


**Figure 4.** The test of the small-world structure. (a) is the 150 results of  $\sigma$ ; (b) is the distribution of the results of  $\sigma$ ; (c) is the 150 results of  $C/C_r$ ; (d) is the distribution of the results of  $C/C_r$ .

algorithm to demonstrate the existence of fractality in many real networks. In accordance with regular fractals, the fractal dimension can be calculated by Box-counting method. The relation between the minimum number of boxes  $N_B(l_B)$  needs to cover the network and the size of the box  $l_B$  follows the power law as follows:

$$N_B(l_B) \sim l_B^{-d_B}. \quad (6)$$

5 If Equation 6 is satisfied by the given network, then  $\log N_B(l_B) \sim -d_B \log l_B$ . Thus, the fractal dimension  $d_B$  can be obtained by  $d_B = -\lim_{l_B \rightarrow 0} \frac{\lg N_B(l_B)}{\lg l_B}$ . In the practical application,  $d_B$  is usually determined by the negative of the slope of line fitted by  $\lg N_B(l_B)$  and  $\lg l_B$  (Molontay, 2015).

The ultimate goal of all box-covering algorithms is to locate the optimum solution, i.e., to identify the  $N_B(l_B)$  value for any given box size  $l_B$ . Song et al. (2007) demonstrated that this problem can be mapped to the graph coloring problem, which was known to belong to the family of NP-hard problems. To solve the problem efficiently, the greedy coloring algorithm is used. As the Song et al. (2005) suggested, the greedy coloring algorithm can both reveal the length-scale invariant topology and determine the fractal exponent. However, a dual network should be constructed beforehand by the application of a renormalization procedure which coarse-grains the system into boxes containing nodes within a given size  $l_B$  (Song et al., 2007). In the greedy coloring algorithm, boxes are treated as the nodes of the dual network. Vertex coloring is a well-known procedure, where colors are assigned to each vertex of a network. Accordingly, the minimum number of boxes  $N_B(l_B)$  is equal to the



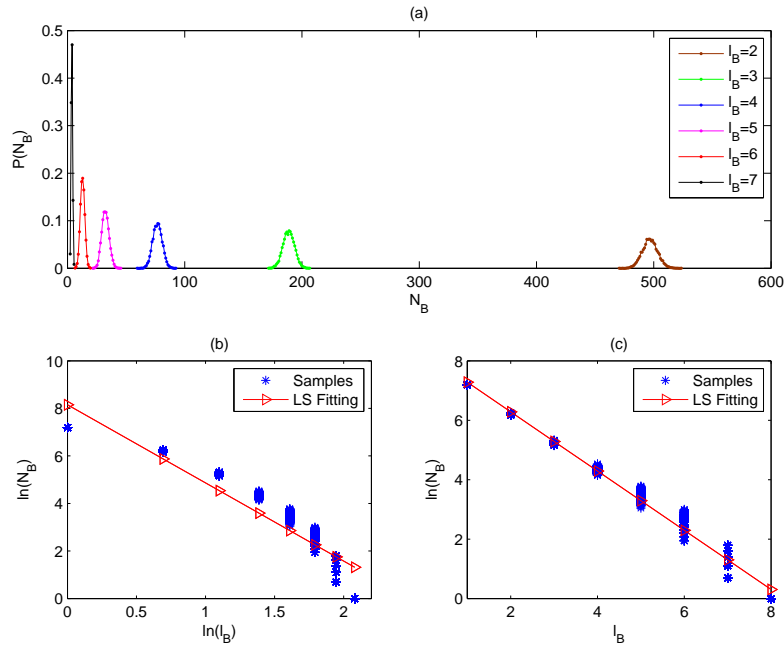


**Figure 5.** The results of 10,000 times of greedy coloring algorithm implementation. (a) The probability distribution function  $P(N_B)$  of the minimum box number of  $N_B$  against different box sizes  $l_B$ ; (b) the 10,000 results of  $N_B$  against different  $l_B$  on the log-log scale and the corresponding Least Square fitting; (c) the 10,000 results of  $\ln(N_B)$  against different  $l_B$  and the corresponding Least Square fitting.

minimum required number of colors. The details of the algorithm is shown in (Song et al., 2007). Because the results of the greedy algorithm may depend on the original coloring sequence, we randomly reshuffle the original coloring sequence and apply the greedy algorithm for 10,000 times to investigate the quality of the algorithm. The results are shown in Figure 5.

Here,  $l_B$  ranges from 1 to  $l_B^{max}$ , which is the maximum distance in the network plus one. Based on the boxing counting algorithm, the distance  $l$  between the nodes in the same box should fulfil  $l < l_B$ . Therefore, when  $l_B$  is 1 and  $l_B^{max}$ , the minimum number of boxes  $N_B$  is the number of node and 1, as is shown in Figure 5 (b) and (c) where  $l_B^{max} = 8$ . Shown in the Figure 5 (a), the distribution curves for all box sizes  $l_B$  are narrow Gaussian distributions, indicating that almost any implementation of the algorithm yields a solution close to the optimal. Accordingly, we can use the mean to stand for the optimal value when we use least square to measure the box dimension  $d_B$ . Comparing Figure 5 (b) and (c), it is obviously that the relationship between  $N(l_B)$  and  $l_B$  follows  $N(l_B) \sim \exp(l_B)$  rather than  $N(l_B) \sim l_B^{-d_B}$ . Therefore, from one year's time length, the ionospheric networks does not have length-scale invariant topology, indicating the complexity of the ionospheric spatial variation for long time. The spatial long-term model's construction of ionosphere is still a challenging work.



#### 4 Conclusions

As an efficient nonlinear approach to describe the spatially extended dynamical systems, complex network is used to analyze the spatial transmission of information in global ionosphere in this paper. As a Bayesian probabilistic graph, the ionospheric information network is constructed based on the conditional independence theory. We have analyzed the topology of the ionospheric network. The results of the power-law hypothesis testing show that both the out-degree and in-degree distribution of the ionospheric networks are not scale-free. None of the spatial position plays a eminently important role in the transmission of ionospheric information. The spatial variation of the ionospheric network shows the connection principally exist between the neighbors in space, indicating that in ionosphere the information flow transmission is mainly based on the nearby principle. Moreover, the spatial distributions of edges show that the information travels further along the latitude than the longitude. Perhaps, this is because the dramatic variation of ionosphere along the geomagnetic field interrupts the information flow. In addition, the small-world structure is studied. The small-world-ness is found to be larger than 1. Meanwhile, the clustering coefficient is larger than those of the classical random graphs. Thus, the ionospheric information network is small-world, which may result from the current system in the ionosphere. Also, the analysis of the length-scale invariant topology shows the ionospheric network is not fractal, indicating the complexity of the spatial variation for long time in ionosphere. In general, the complex network provide a peculiar perspective for the ionosphere research. Depending upon the choice of nodes and/or edges and/or methods, ionospheric networks may take different forms to study different property of ionosphere.

*Code availability.* Code are available by email request.

*Data availability.* VTEC data is derived from CODE (<ftp://ftp.unibe.ch/aiub/CODE>) in the form of Global Ionospheric Map.

*Competing interests.* No competing interests are present

20 *Acknowledgements.* This work was supported by the National Natural Science Foundation of China (41374154). We are grateful to Adam Woods from CIRES, University of Colorado, David Skaggs Research Center, Rolf Dach and Stefan Schaer from Astronomical Institute, University of Bern. They are all so kind to help us on the data obtaining.



## References

- Abe, S. and Suzuki, N.: Complex-network description of seismicity, *Nonlinear Processes in Geophysics*, 13, 145–150, 2006.
- Abe, S. and Suzuki, N.: Main shocks and evolution of complex earthquake networks, *Brazilian Journal of Physics*, 39, 428–430, 2009.
- Baiesi, M. and Paczuski, M.: Complex networks of earthquakes and aftershocks, *Nonlinear Processes in Geophysics*, 12, 1–11, 2005.
- 5 Barabási, A. L. and Albert, R.: Emergence of Scaling in Random Networks, *Science*, 286, 509, 1999.
- Clauset, A., Shalizi, C. R., and Newman, M. E. J.: Power-Law Distributions in Empirical Data, *Siam Review*, 51, 661–703, 2009.
- Donges, J. F., Zou, Y., Marwan, N., and Kurths, J.: The backbone of the climate network, *Europhysics Letters*, 87, 48 007–48 012, 2009a.
- Donges, J. F., Zou, Y., Marwan, N., and Kurths, J.: Complex networks in climate dynamics - Comparing linear and nonlinear network construction methods, *The European Physical Journal Special Topics*, 174, 157–179, doi:10.1140/epjst/e2009-01098-2, 2009b.
- 10 Ebert-Uphoff, I. and Deng, Y.: A new type of climate network based on probabilistic graphical models: Results of boreal winter versus summer, *Geophysical Research Letters*, 39, 19 701, 2012.
- Ercha, A., Huang, W., Yu, S., Liu, S., Shi, L., Gong, J., Chen, Y., and Hua, S.: A regional ionospheric TEC mapping technique over China and adjacent areas on the basis of data assimilation, *Journal of Geophysical Research: Space Physics*, 120, 1–13, doi:10.1002/2015JA021140, 2015.
- 15 Gallos, L. K., Song, C., and Makse, H. A.: A review of fractality and self-similarity in complex networks, *Physica A Statistical Mechanics & Its Applications*, 386, 686–691, 2007.
- Guo, J., Li, W., Liu, X., and Kong, Q.: Temporal-Spatial Variation of Global GPS-Derived Total Electron Content 1999-2013, *PLOS ONE*, 10, 1–21, doi:10.1371/journal.pone.0133378, 2015.
- Hlinka, J., Hartman, D., Vejmelka, M., Runge, J., Marwan, N., Kurths, J., and Palu, M.: Reliability of Inference of Directed Climate Networks Using Conditional Mutual Information, *Entropy*, 15, 2023–2045, 2013.
- 20 Humphries, M. D. and Gurney, K.: Network 'small-world-ness': a quantitative method for determining canonical network equivalence., *Plos One*, 3, e0002 051, 2008.
- Humphries, M. D., Gurney, K., and Prescott, T. J.: The brainstem reticular formation is a small-world, not scale-free, network, *Proceedings of the Royal Society B Biological Sciences*, 273, 503, 2011.
- 25 Jie, C., Russell, G., Jonathan, K., David, B., and Weriu, L.: Learning Bayesian networks from data: An information-theory based approach, *Artificial Intelligence*, 137, 43–90, 2002.
- Jiménez, A., Tiampo, K. F., and Posadas, A. M.: Small world in a seismic network: the California case, *Nonlinear Processes in Geophysics*, 15, 389–395, 2008.
- Kelly, M.: *The Earth's Ionosphere: Plasma Physics and Electrodynamics*, Academic Press(Elsevier), 2nd edn., 2009.
- 30 Koller, D. and Friedman, N.: *Probabilistic Graphical Models: Principles and Techniques - Adaptive Computation and Machine Learning*, MIT Press, 2009.
- Molontay, R.: *Fractal Characterization of Complex Networks*, 2015.
- Murphy, K. P.: *Machine Learning: A Probabilistic Perspective*, MIT Press, 2012.
- Newman, M.: *Networks: An Introduction*, Oxford University Press, Inc., 2010.
- 35 Nihat, A. and Daniel, P.: Information flows in causal networks, *Advances in Complex Systems*, 11, 17–41, 2011.
- Nocke, T., Buschmann, S., Donges, J. F., Marwan, N., Schulz, H. J., and Tominski, C.: Review: visual analytics of climate networks, *Nonlinear Processes in Geophysics*, 2, 709–780, 2015.



- Peron, T. K. D., Comin, C. H., Amancio, D. R., Costa, L. D. F., Rodrigues, F. A., and Kurths, J.: Correlations between climate network and relief data, *Nonlinear Processes in Geophysics Discussions*, 1, 1127–1132, 2014.
- Phillips, J. D., Schwanghart, W., and Heckmann, T.: Graph theory in the geosciences, *Earth-Science Reviews*, 143, 147–160, 2015.
- Podolská, K., Truhlík, V., and Trísková, L.: Analysis of ionospheric parameters using graphical models, in: EGU General Assembly Conference, 2010.
- 5 Podolská, K., Truhlík, V., and Trísková, L.: Study of Correlations between Main Ionospheric Parameters by Stochastic Modeling, in: EGU General Assembly Conference, 2012.
- Ramsey, J., Glymour, M., Sanchezromero, R., and Glymour, C.: A million variables and more: the Fast Greedy Equivalence Search algorithm for learning high-dimensional graphical causal models, with an application to functional magnetic resonance images, *International Journal of Data Science & Analytics*, 3, 121, 2017.
- 10 Song, C., Havlin, S., and Makse, H. A.: Self-similarity of complex networks., *Nature*, 433, 392, 2005.
- Song, C., Gallos, L. K., Havlin, S., and Makse, H. A.: How to calculate the fractal dimension of a complex network: the box covering algorithm, *Journal of Statistical Mechanics Theory & Experiment*, 2007, 297–316, 2007.
- Suteanu, M.: Scale free properties in a network-based integrated approach to earthquake pattern analysis, *Nonlinear Processes in Geophysics*, 15 21, 427–438, 2014.
- Wang, J., Jiang, C., Quek, T. Q., and Ren, Y.: The Value Strength Aided Information Diffusion in Online Social Networks, in: IEEE Global Conference on Signal and Information Processing (GlobalSIP), pp. 1–6, Washington, DC, USA, 2016a.
- Wang, J., Jiang, C., Quek, T. Q., Wang, X., and Ren, Y.: The Value Strength Aided Information Diffusion in Socially-Aware Mobile Networks, *IEEE Access*, 4, 3907–3919, 2016b.
- 20 Watts, D. J. and Strogatz, S. H.: Collective dynamics of 'small-world' networks., *Nature*, 393, 440, 1998.
- Wei, N., SHI, and Zou, R.: Analysis and Assessments of IGS Products Consistencies, *Geomatics and Information Science of Wuhan University*, 34, 1363–1367, doi:1671-8860(2009)11-1363-05, 2009.
- Zerenner, T., Friederichs, P., Lehnertz, K., and Hense, A.: A Gaussian graphical model approach to climate networks., *Chaos An Interdisciplinary Journal of Nonlinear Science*, 24, 47, 2014.